《生物科学杂志》

Journal of Biological Sciences

ChengZhu Science™

江西省诚筑环保工程有限公司主办

2022 年 11 月刊物/Serial in November, 2022

出版人： 刘焕 香江出版社有限公司

Publisher: Liu Huan, Xiangjiang Publishing Company Ltd.

Copyrights Statements

Copying and Transferring is Forbidden!

版权申明

禁止复制、转载！

Article 13. Essay: Structural Molecular Biology

Author: Liu Huan (1983-), Master of Science (First Class Honours, 2009), The University of Auckland.

DOI:10.58473/JBS0021 Retrieval from official database: www.crossref.org

Latest revised on 05/06/2023.

Summary of Key Features

The limitations of DNA sequencing technology have been critically discussed in my previous article of this journal. Instead, the molecular structural biology becomes the alternative technology to further characterize the genetic information in more exact way, which focus on the spatial distribution of DNA sequences inside DNA structure. A novel method of DNA structure observation is presented in my previous article, which is convenient and cheaper cost for practical application. In comparison, bio-markers of molecular structural biology achieves the classification of genetic information at the chromosome/genome level which is more specific, while the DNA sequencing markers stay in the identification of genetic information at the cellular levels. However, by fully summarizing case studies on structural biology, it is realized that fewer studies choose DNA molecules to observe, while most of case studies target protein species as study purpose, consequently becoming the new research gaps in future structural biology study.

Key words: Structural biology, The primary structure, The secondary structure, The tertiary structure, DNA marker.

1. Introduction

Since nanotechnology has been globally developed in 1980s, various technologies are designed to observe the macro-bio-molecules in three dimensions. This article firstly outlines the comprehensive study content of structural biology, trying to summarize all the relevant conceptions in understanding this theme. Then the commonly used technologies on structural biology are illustrated by case studies as comparison and contrast, to identify the research gaps in structural biology for future studies.

2. Study content of structural biology

In order to achieve its own biological function, each species of bio-molecules must meet two pre-conditions. First, all biological macromolecules that function actively must possess the specific, unique and relatively stable tertiary structure. Second, structural motions among biological molecules are required. Consequently, structural

biology emphasizes on the tertiary structure of bio-macromolecules as the methods to study the relationship/mechanism between the structure and function of biological macromolecules. The instruments used in structural biology mainly include X-ray crystallography, nuclear magnetic resonance spectroscopy, electron microscopy and other physical technologies to study the function and structure of biological macromolecules [1].

The tertiary structure of biological macromolecules are summarized into tertiary DNA structure, tertiary RNA structure and quaternary protein structure separately below as contrast and comparison.

2.1. The primary structure of DNA molecule

The primary DNA structure is the original deoxynucleotide chain formed by arranging deoxynucleotides in orderly sequences, which determines the type and amount of genetic information.The primary structure is the basis of the advanced structure of DNA, but the change of the primary structure does not essentially alter the advanced structure that influences the function of DNA [2].

2.2. The secondary structure of DNA molecule

1. Two polynucleotide chains integrate a right-handed double helix around the same and common axis with the consistent rotation, in which the diameter of the helix is approximately 2.0 nm; 2. Two polynucleotide chains are reverse parallel, where one is 5'-3' and the other is 3'- 5'; 3. The sugar phosphate skeleton of the two polynucleotide chains is located outside the double helix, while the base plane is located inside the chain; 4. The axial distance of each helix is 3.4 nm, in which the axial distance between adjacent base pairs is 0.34 nm [3].

2.3. The tertiary structure of DNA molecule

On the basis of double helix, DNA molecules further twist around the same central axis to create additional helix, and this extra helix of the ring molecule forms a super helix, which can be either a right-handed helix (known as positive super helix) or a left-handed helix (known as negative super helix). Other forms of tertiary DNA structure include the complex of DNA molecules directly binding to protein as advanced structure, and nucleosome structure of eukaryotic chromosomes binding to histone [4].

2.4. The primary structure of RNA molecule

DNA is constructed from deoxyribonucleotides, while RNA is composed of ribonucleotides, in which an oxygen atom is added to the 3 ' carbon atom of the ribose sugar ring. In all base pairs, base pair u (uracil) of RNA molecule replaces thymine in DNA molecule. The primary structure of RNA is the orderly sequences of ribonucleotides chain, which gives broader scope forming folding structure than DNA molecules [8].

2.5. The secondary structure of RNA molecule

The secondary structure of RNA is determined by base pairs. In addition to the common base pairs of Watson-Crick, mismatched base pairs can also be found, such as GU base pairs. The secondary structure is constructed by hydrogen bonds containing an energy of about -12kJ / mol. The accumulation of base pairs makes an energy contribution of about -23kJ / mol, giving the most stable conformation. However, the stacking energy of base pairs is not symmetrical, and the energy contribution of GC stacking on AU is different from that of stacking on GC [8].

2.6. The tertiary structure of RNA molecule

The most complex structural level is the tertiary structure. Tertiary structure is mainly the spatial arrangement of secondary structure, such as stem-loop structure. There are several types of forces forming tertiary structure of RNA molecules: a coil can form a hydrogen bond with another part of the structure to stabilize it. In addition, van der Waals force and electrostatic force also contribute greatly to the tertiary structure. Finally, protein molecules can interact with RNA tertiary structure and stabilize it. However, RNA chains, like most polypeptide chains, do not form topology[8].

2.7. The primary structure of protein molecule

The primary structure in each protein molecule contains the sequence of amino acids in the polypeptide chain, which includes the amount of polypeptide chains consisting of the protein and the amino acid sequence in polypeptide chain, as well as the position of disulfide bond. The primary structure of the protein is also known as the basic structure in protein molecule [5].

2.8. The secondary structure of protein molecule

The secondary structure of protein molecule is the spatial structure of a certain peptide chain in protein molecule, which reveals the relative spatial position of the main peptide chain against the whole protein molecule, but does not involve the structure of the side chain of amino acid residues. The secondary structure measured exists in all proteins species. The main forms include: a-helix, β-Folding, β-Corner, random curl, etc [6].

2.9. The tertiary structure of protein molecule

A polypeptide chain based on the secondary structure, super secondary structure or structural domain leads to various tortuous and folding structures in protein molecules due to the interaction of side chains of amino acid residues apart to its peptide chain, forming the spatial arrangement including main and side chains. This overall three-dimensional array and structure of all atoms along a polypeptide chain is called tertiary structure of protein [7].

2.10. The quaternary structure of protein molecules

Globulin molecules with larger molecular weight often contain two or more polypeptide chains. These polypeptide chains themselves have a spherical tertiary

structure, which are linked to each other by secondary bonds (including hydrogen bonds, hydrophobic interactions and salt bonds) to form a stable structure. These independent secondary bonds are the subunits of protein molecules, whose type, amount, spatial distribution and mutual interaction consists of quaternary structure of protein molecules [9].

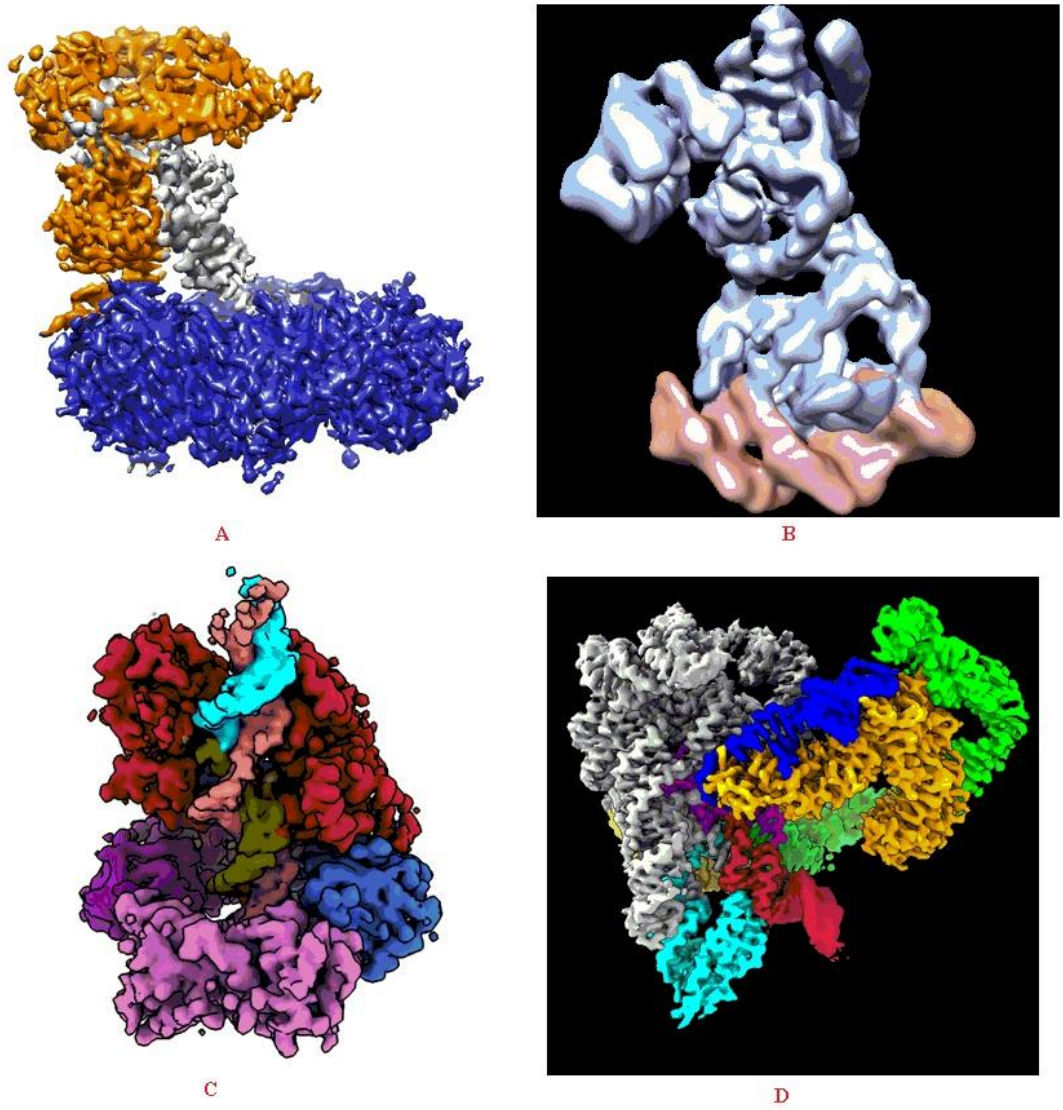

Figure 1. Tertiary structure of DNA. Figure A is the Cryo-EM multiframe micrographs of human Pol kappa complexed with DNA and wildtype PCNA (DOI: 10.6019/EMPIAR-10933); Figure B is CryoEM single particle dataset for NanR dimer-DNA hetero-complex (DOI:10.6019/EMPIAR-10836); Figure C is Archaeal DNA ligase and heterotrimeric PCNA with non-ligatable nicked DNA (DOI: 10.6019/EMPIAR-11551); Figure D is CryoEM micrographs of a group II intron retroelement in complex with its structured DNA target (holoRNP) (DOI: 10.6019/EMPIAR-11315). **All the figure data source from EMPAIR with Public domain licenses to re-use** [44][45][46][47][48].

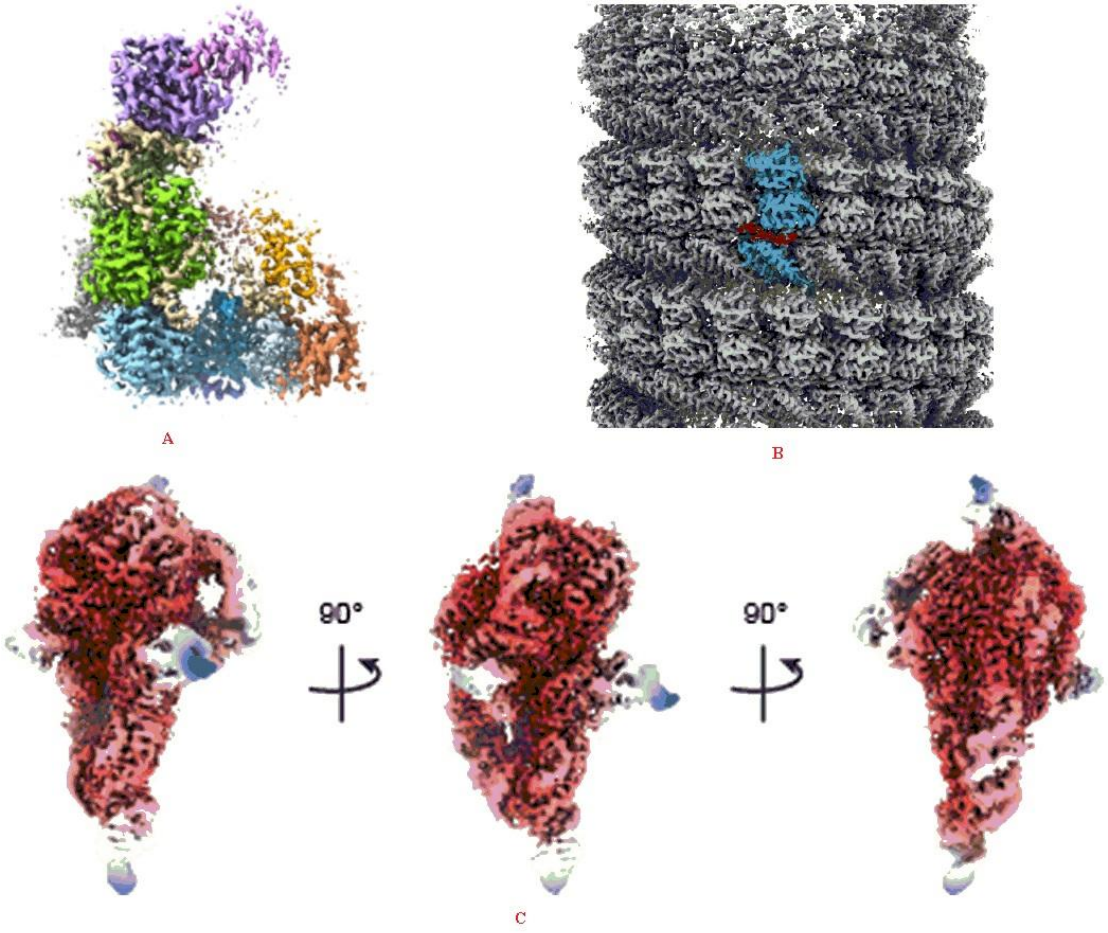

Figure 2. Tertiary structure of RNA. Figure a is Structure of the Dicer-2-R2D2 heterodimer bound to a small RNA duplex (DOI:10.6019/EMPIAR-11099); Figure B is Lloviu cuevavirus nucleoprotein RNA complex (DOI:10.6019/EMPIAR-11323); Figure C is E.coli RNaseP ES complex with AU_ptRNA substrate in the presence of Ca2+ (DOI:10.6019/EMPIAR-11334). **All the figure data source from EMPAIR with Public domain licenses to re-use** [49][50][51].

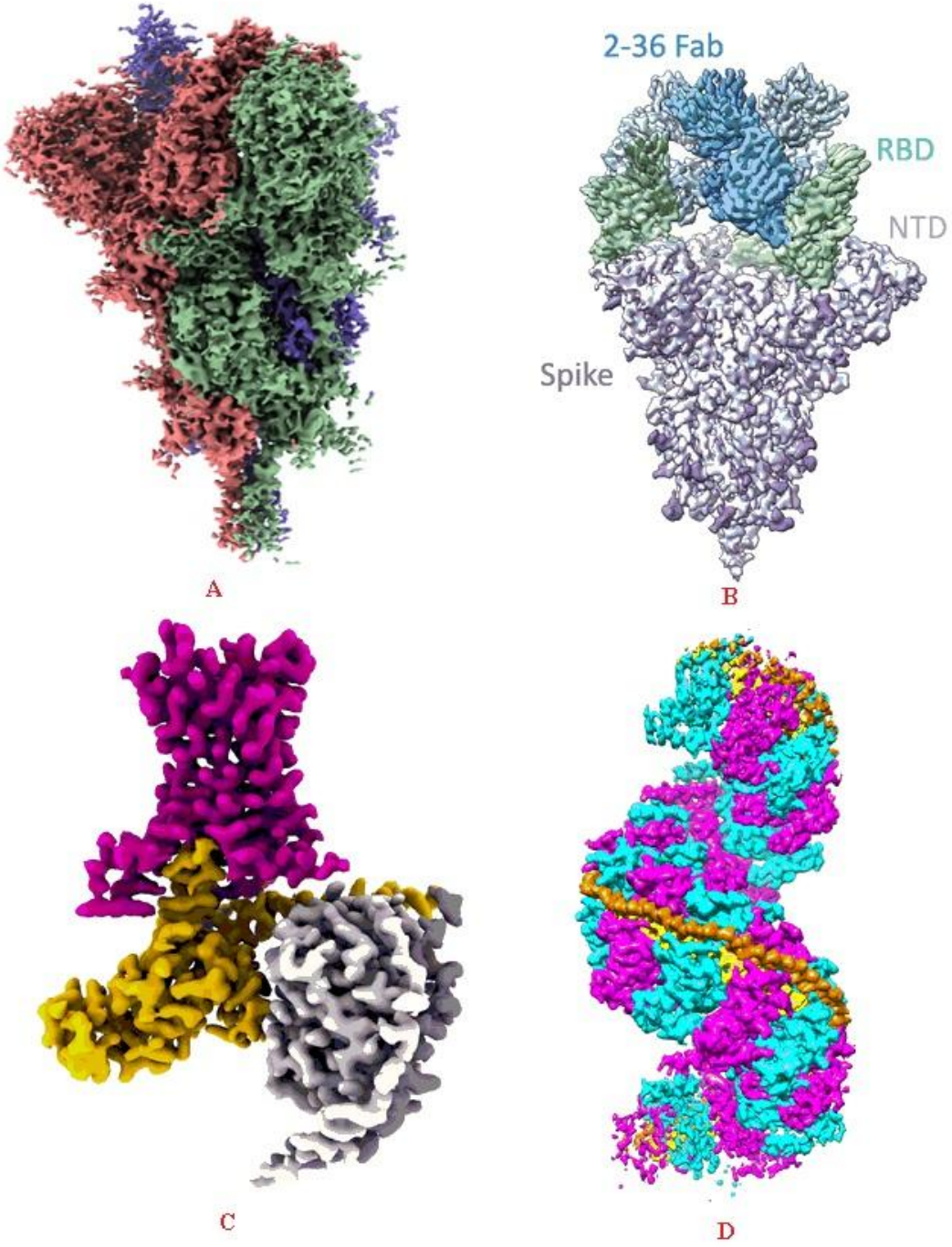

Figure 3. Tertiary structure of Protein. Figure A is SARS-CoV-2 spike protein (1-up RBD) on EG-grid (DOI: 10.6019/EMPIAR-10951); Figure B is Cryo-EM SPA datasets of broadly neutralizing antibody 2-36 in complex with prefusion SARS-CoV-2 and SARS-CoV spike glycoproteins (K3 movies/.tif files) (DOI: 10.6019/EMPIAR-11513); Figure C is LPHN3 (ADGRL3) 7TM domain bound to tethered agonist in complex with G protein heterotrimer (DOI: 10.6019/EMPIAR-11432); Figure D is Structure of RecT protein from Listeria

innoccua phage A118 in complex with 83-mer annealed duplex (DOI: 10.6019/EMPIAR-11348). **All the figure data source from EMPAIR with Public domain licenses to re-use** [52][53][54][55].

3. Nano-Technology applied to structural biology

In total 9 types of nano-technologies which are commonly used in structural biology studies have been summarized in this part, giving representative case studies to illustrate each technology, which are outlined in Table 1.

3.1. X-ray diffraction by crystals

The crystal displays the lattice structure, and the circle of the lattice structure (i.e. structural unit of cell length) shows the same order of magnitude as the wavelength of X-ray. X-ray diffraction is an interference phenomenon based on the principle of wave superposition, and the interference types vary with different optical path difference.When the length of optical path difference is the even times of half wavelength, the amplitude of synthetic wave is the largest; when the length of optical path difference is the odd times of half wavelength, the synthetic amplitude is zero. Therefore, after X-rays penetrates into and converts through the crystal, the intensity of X-rays in some directions (diffraction direction) increases, while the intensity of X-rays in other directions may decrease or even disappear. If a photosensitive film is placed behind the crystal, the diffraction pattern of X-rays will be obtained [10].

The X-ray diffractometer made by using the principle of X-ray diffraction is the most important instrument for detecting the crystal structure. Lattice parameters, mainly including the size and shape of crystal cells, can be determined according to the direction of diffraction. Based on the diffraction intensity distribution, the coordinates of atoms in the crystal cell can be also measured, which is also the main method to analyze the molecular space configuration[10]. For example, protein crystallography focuses on the three-dimensional structures of macro bio-molecules at atomic resolution, which has been broadly applicable on both academic laboratories and the pharmaceutical industry in the past. The investigating of three-dimensional atomic structures in proteins contributes to the design of new drugs or the improvements of existing drug functions [20].

Shi (2019) conducted research on acetylation by using X-ray diffractometer, a post-translational modification of protein that widely existed in eukaryotic and prokaryotic cells. Under the catalysis of acetyltransferase, acyl donors (such as acetyl CoA and other small molecular compounds) converted acetyl groups into the relevant amino acid residues of substrate proteins. ElaA protein was widely distributed in a variety of bacteria and shows high homology in different strains. In this study, ElaA (EcElaA) from E. coli K-12 strain was selected to analyze its three-dimensional

structure and functional relationship. Through large-scale expression and purification of EcElaA, the purified protein was screened by crystallization, to obtain crystals with X-ray diffraction quality. By collecting diffraction data, it was to analyze the crystal structure reaching a resolution of 2.60A. The structure showed that EcElaA possessed the typical structural characteristics of GCN5-relatedN-acetyltransferase （GNAT）family, which consisted of seven inverse-parallel elements of β Folding and 4 pieces of α- Spiral composition. Through structural comparison, it was also found that the three-dimensional conformation of SACOL1063-AcCoA complex, as another member of GNAT family from Staphylococcus aureus, was highly similar to EcElaA, which showed similar acetyl CoA binding sites and receptor substrate binding sites. After ultracentrifugation analysis, it was known that EcElaA mainly existed in the form of dimer in the solution, and the isothermal titration calorimetry (ITC) results showed that there was an obvious interaction between small molecule Acetyl CoA (AcCoA) and EcElaA. However, when the crystals of EcElaA - AcCoA complex was screened after a lot of crystallization optimization, is was failed to obtain crystals of X-ray diffraction quality [18]. This would indicate that EcElaA - AcCoA complex is not the stable form of biological molecules.

The spatial arrays of collagen fibrils and apatite crystals, which were abstracted from a bony fish (*Leuciscus cephalus*), were studied and observed by X-ray diffraction. The diffraction arrays at each specific angle was observed clearly by using a micro-focus scanning setup, which integrated the collagen reflections at five selected orientations with an interval of 36° among each other orientation. In addition to the electron microscopic methods examining plywood arrangements in both calcified and uncalcified tissues, these results were the first diffraction data that further supported the existence of these peculiar structures, so that it represented a promising tool to investigate plywood displaying in biological tissues [19].

As comparison and contrast to detecting the crystal structure, the Coherent X-ray diffraction imaging (CXDI) was recently developed to discover the non-crystalline bio-particles at resolution from micrometer to sub-micrometer. A diffraction apparatus was applied on single-shot CXDI experiments to study the non-crystalline bio-particles in frozen-hydrated state, which was under cryogenic temperature concurrently by using X-ray free electron laser pulses, and the future application of this instrument was discussed by developers [21].

3.2. Nuclear magnetic resonance (NMR)

The principle of nuclear magnetic resonance is mainly caused by the rotation motion of atomic nucleus. Different nuclei show different rotation motions, which can be expressed by spin quantum number (I) of the nucleus that is influenced by atomic mass and atomic number. If a nucleus achieves the transition from low-energy state to high-energy state, this nucleus must absorb the energy of △E from the external electromagnetic waves of certain frequencies. When the emitted radiation energy by

external instrument exactly reaches the required and absorbed energy △E, the spin nucleus in the low-energy state transitions to the high-energy state. This phenomenon is called nuclear magnetic resonance (NMR) [11].

Although the accuracy of NMR technology determining the three-dimensional structure of biological macromolecules is not as high as that of X-ray derivation method, it gives the advantages that X-ray derivation method does not have: firstly, NMR method can study the three-dimensional structure of biological macromolecules in aqueous solution or organic phase; secondly, NMR method can study the influence of aqueous solution on the structure of biological macromolecules by adjusting its environmental conditions. The environmental factors of aqueous solution are wide, mainly including pH, ion concentration, temperature, reaction substrate, products, activator, inhibitor, denaturant etc [9].

Zeng (2013) used nuclear magnetic resonance (NMR) as the main method to study two polypeptides that were important to cell membrane fusion and transmembrane signal in transduction function, which demonstrated the application of NMR technology on investigating macro bio-molecules. The first study objective was to understand the structure and membrane fusion mechanism of baculovirus envelope protein F protein fusion peptide, which was the inevitable pathway for viruses to invade host cells. The fusion peptide of *Helicoverpa armigera* nuclear polyhedrosis in virus F protein (HAF) was investigated by NMR to reveal the structure of its four mutants with different fusion functions (d11l, I2n, N1G, G3l), in comparison to the homologous wild-type gypsy moth nuclear polyhedrosis virus F protein (ld130) fusion peptide. The relationship between the structure and function of baculovirus fusion peptide was summarized, with the details of the binding state of each peptide to micelles by further conducting paramagnetic broadening experiment. The HAF fusion peptide of wild-type baculovirus showed a regular and representative inverted 'V' (or boomerang) structure in the membrane system. More detailed information were examined with regards to the three-dimension structure of protein molecules, which further speculated that the structure of baculovirus fusion peptide was divided into two types of 'fusion region' and 'structural region', resulting in the membrane insertion [22].

Wu (2010) conducted research on the cloning, expression and purification of UBX domain of human UBXD2 protein by using liquid NMR, and the interaction between UBXD2 protein and VCP protein was preliminarily studied. According to the structure obtained by parsing, the spatial structure of UBXD2 UBX domain included 2 segments of α Spiral and 4 segments of β, forming folds with a loop area closely related to its function. A hydrophobic core were constituted by 2 α Spiral and 4 segments β Hydrophobic residues between folds, maintaining the stability of protein. Through further experiment of homologous sequence alignment, it was found that the loop region closely related to its function was conservative, with an FP motif for binding. In the process of parsing, two of the six prolines contained in UBXD2 UBX

domain were in cis conformation, one of which was located at the key binding site FP motif. By conducting chemical shift interference experiment, the interaction between UBXD2 UBX domain and VCP VCP-N domain was identified to be relatively weak, showing fast exchange. Due to the relatively conservative tertiary structure of UBX domain, bioinformatics methods was used to model the complex structure of UBXD2 UBX domain and VCP VCP-N domain, by referring to the UBX domain P47 UBX and VCP VCP-ND1 protein in the protein database by computer. Secondly, this research used NMR to understand the interaction between dendrimers and deoxycholic acid, a bioactive surfactant. It was found that deoxycholic acid molecules were only located in the hydrophobic pocket of dendrimers without binding to the surface, revealing that the combination between dendrimers and deoxycholic acid was caused by both hydrophobic interaction and hydrogen bond interaction between them. Further more, based on the study of the interaction between dendrimers, deoxycholic acid and chaps, the conventional and new NMR techniques were applied to screen the drugs based on dendrimer binding, which helped to design different schemes to deal with the high-throughput screening of dendrimer insoluble drugs and dendrimer soluble drugs, leading to a set of NMR methods for high-throughput drug screening[23].

3.3. Electron microscope three-dimensional reconstruction technology

Electron microscope three-dimensional reconstruction is a new technology with important application prospects, which is achieved by the combination of electron microscopy, electron diffraction and digital image processing. It is especially suitable for analyzing the three-dimensional structure of membrane proteins that are difficult to form three-dimensional crystals and large complexes, such as viruses and protein nucleic acid complexes. The basic step is to take photos of biological samples at different angles in the electron microscope, obtain a series of electron microscope pictures, and then process them by Fourier transform, so as to show the electron density map of the three-dimensional structure of biological macromolecules and their complexes [12].

Freeze electron microscopy has become a powerful tool to study the structure and function of biological macromolecules since this technology developed. This method uses high-pressure and rapid freezing method by liquid nitrogen to embed the sample under the glassy water environment, which is closer to the physiological state, reducing the structural damage of the sample in the preparation process, so that we can observe the structure of biological macromolecules in the natural state. At the same time, the freezing speed is very fast, which may fix the cells at some specific moments of their physiological activities (such as muscle contraction), and then show the structural characteristics at this transient time, so that the functions of biological molecules can be studied through the instantaneous conformational changes of different functional states. The two-dimensional projection images of molecules in natural state without staining were obtained by freezing electron microscope. The data obtained by tilting the sample at different angles are comprehensively analyzed, and

the three-dimensional molecular structure is obtained by using different reconstruction techniques according to the different characteristics of the sample [12]. Other treatment methods embed the bio-samples include negative staining, glucose embedding, tannic acid embedding [9].

Candida albicans is the typical pathogen to patients with AIDS, cancer and other diseases causing immune deficiency. Pral, as an endogenous complement protein inhibitor expressed by *Candida albicans*, plays a key role in the immune escape of *Candida albicans,* through inhibiting the activation of alternative pathway (AP) by cleaving complement protein C3. The molecular mechanism of C3 cleavage by Pral was analyzed by three-dimensional reconstruction technology of electron microscope. First, it was to predict and analyze the structural characteristics of Pral monomer by homology modeling. Then, the purified C3 protein extracted from plasma was reconstructed by negative staining electron microscope single particle technology, and the three-dimensional structural model of C3 protein in natural state was obtained; Finally, it was to explore the formation conditions of C3 Pral complex, taking concentration ratio, incubation temperature and incubation time as variables, to determine the optimal conditions for electron microscopic observation of C3 Pral complex [24].

Virus particles usually possess large molecular weight which are difficult to crystallize, so that cryoelectron microscopy is the most powerful tool to analyze the virus structure that is not required to crystallize the sample. Virus particles generally display high symmetry (such as icosahedral symmetry) which is used to suppress image noise and improve the resolution of final reconstruction. Song (2021) developed a new local reconstruction method based on the three-dimensional reconstruction of icosahedron cryoelectron microscope, which partially refined and reconstructed the flexible protein region to obtain the structure of high-resolution flexible protein. Firstly, the high-resolution structure of human adenovirus capsid
3.4 Å was obtained by using icosahedral three-dimensional reconstruction technology, with the atomic model based on the three-dimensional density map; Secondly, the method of partially refinement and reconstruction was developed, written and edited by a large-scale calculation program package; Thirdly, several flexible small proteins (IX, VII, IIIA) on the human adenovirus capsid were regionally reconstructed with high-resolution structure, and their corresponding atomic models were modified [25].

3.4. Biological mass spectrometry

Biological mass spectrometry becomes the main supporting technology of protein identification and analysis. It analyzes the composition and structure by measuring the ratio of mass to charges (m/z) in sample ions [13]. There are three common methods used:

Firstly, matrix assisted laser desorption ionization time of fight MS (MALDITOF-MS) is to mix and co-crystallize the sample with small molecular matrix (such as cinnamic

acid, erucic acid and their derivatives). When UV laser (337nm) irradiates the crystal, the matrix molecules absorb energy to desorb and ionize the sample with matrix molecules. The ions produced by the sample obtain the same kinetic energy under the action of accelerating electric field. After passing through a vacuum electric field pipe for free flight, the lighter ions have a faster speed and arrive at the detector earlier, while the heavier ions arrive at the detector later. The flight duration is proportional to m/z. The majority of ions produced by MALDI are single charged ions, and the spectral peaks in the mass spectrum have a one-to-one correspondence with the ion mass of each component of sample. Therefore, MALDI-MS is suitable for analyzing peptide mixtures after protein hydrolysis [13].

Secondly, electrospray spray ionization mass spectrometry (ESIMS) uses high voltage to charge the droplets from the capillary column at the mass spectrometry injection end. Under the effects of reverse N_2 gas flow, the droplet solvent evaporates, leading the surface to shrink, the surface charge density continues to ascend, which further makes the droplet burst into charged sub-droplets. This process continues to repeat, making the final droplet very tiny in the form of spray. At this state, the voltage on the droplet surface is very strong to ionize the analyte, which enters the mass analyzer in the form of single or multi charged ions. The mass spectrum peak corresponds to a series of m/z peaks with different charges of this compound, which can be converted into molecular ion peaks with single charge by software calculation [9][13].

Thirdly, tandem mass spectrometry (MS/MS) selectively analyzes the component surface in a mixture without separating each group. The first level mass analyzer obtains all components from the peak parental ion, and selects the parental ion that needs to be analyzed in the sample through the mass escape device. This parent ion generates fragment ions (sub-ions) through collimation induced dissociation (CID) of high flow speed inert gas in the collision room, and then the sub ions enter the second level mass analyzer to obtain the fragment peak of the parent ion. The structural information of peptides and proteins can be obtained by studying the cleavage relationship between parental ions and sub - ions [9][13].

Zhang et al.,(2015) differentiated the protein expression between normal leukocytes and acute leukemia (AL) cells, and the unique protein expression profiles among various sub-types of AL cells from 61 patients were specified on the basis of FAB schemes using the improved biological mass spectrometry and two-dimensional gel electrophoresis. The results showed that the optimized mass spectrometry and two-dimensional gel electrophoresis played a key role in the accurate identification of proteins at low abundance. This research firstly found that myeloid associated proteins 8 and 14 could be used to indicate the degree of differentiation in acute myeloid leukemia (AML), which consequently distinguished AML from acute lymphoblastic leukemia (ALL); Heat shock protein 27 and other proteins highly expressed in ALL clearly distinguished AML from ALL; NM23 protein related to prognosis was found to be low expressed in M3a, but high expressed in M3b and

other leukemia sub-types; AL cells of different sub-types were classified according to FAB schemes with unique protein expression in morphological characteristics. These findings were of significance for the diagnosis, classification and prognosis of clinical leukemia and drug target research, already leading to patents [26].

A serological method for the diagnosis of esophageal cancer was established based on magnetic bead separation and biological mass spectrometry by Liu et al., (2012). In total 123 serum samples (including 63 cases of esophageal cancer and 61 cases of normal people) were randomly divided into modeling group and validation group. The serum protein mass spectra between esophageal cancer and normal people were established by using matrix assisted laser desorption / ion time of flight mass spectrometry (MALDI-TOF-MS), combined with magneticbead-weak cation exchange (MB-WCX). Clinpro tools 2.2 software was used to quantitatively differentiate the serum protein mass spectra of 32 patients with esophageal cancer from 30 normal people in the modeling group, resulting in the supportive vector machine algorithm used to establish a diagnostic model for esophageal cancer. Then the obtained diagnostic model was used to classify and diagnose the samples in the validation group (31 patients with esophageal cancer and 31 normal people) to evaluate the diagnostic value of the diagnostic model. By comparing and analyzing the serum protein mass spectra between esophageal cancer and normal people, the results showed that there were 21 differential protein peaks ($P < 0.05$), of which 12 were up-regulated and 9 were down-regulated in esophageal cancer. Three differential peaks (MR 654.74, 1451.48 and 1866.67 Dr, respectively) were used to establish a diagnostic model, achieving sensitivity of 93.75% (30/32) and specificity of 90.00% (27/30) respectively. After double-blind verification of independent samples, the sensitivity was 93.55% (29/31) and the specificity was 90.32% (28/31) respectively, approximately equal to the modeling results, showing that this diagnostic model was effective [27].

3.5. Microcalorimetry

Microcalorimetry determines various thermodynamic and kinetic parameters, such as specific heat capacity, enthalpy change, reaction heat, phase diagram, reaction rate, crystallization rate, polymer crystallinity, sample linearity, etc, which shows the following characteristics [14][9]:

Firstly, it does not interfere with the physiological functions of proteins and nucleic acids, and possesses a unique non-specific advantage, which means that there are no restrictions on the solvent properties, spectral properties and electrical properties of the studied protein and nucleic acid system [14][9].

Secondly, the sample dosage requirement is tiny, and the method is highly sensitive, so there is no need to make a transparent and clear solution during measurement [14][9].

Thirdly, the sample after calorimetric test is not damaged, so that subsequent biochemical analysis can be carried out [14][9].

Fourthly, microcalorimetry lacks specificity. However, due to the specificity of proteins and nucleic acids, this non-specific method can sometimes get results that cannot be obtained by specific methods as supplementary methods [14][9].

Wang et al.,(2020) developed a rapid method for real-time determination of antibacterial effects in vitro based on isothermal microcalorimetry, and comparison of the antibacterial effect between the original (Roche Fen) and the imitation (MY) ceftriaxone sodium in vitro was conducted. By using *Staphylococcus aureus* as the target bacterial strain, the effects of the original ceftriaxone sodium and the imitation ceftriaxone sodium on the growth and metabolism of *Staphylococcus aureus* were compared by microcalorimetry test, which were quantitatively evaluated by using the thermal parameters of the expression power - time curve (thermogram curve), including Growth Rate Constant K, Maximum Thermal Power PM, Time of the Main Peak on the thermogram curve and Passage Time TG. In order to verify the conclusion of isothermal microcalorimetry test, the antibacterial activities of both the original and the imitation ceftriaxone sodium were further tested by tube disk method and high performance liquid chromatography (HPLC). Results showed that both the original ceftriaxone sodium and the imitation ceftriaxone sodium expressed bacteriostatic activity, but the bacteriostatic effect of the original ceftriaxone sodium was more obvious than the imitation ceftriaxone sodium, which was consistent with the test conclusion of both traditional tube plate method and HPLC method. However, the isothermal microcalorimetry experiment only taken 24 hours, while both the tube dish method and HPLC method required more than 48 hours. Consequently it was concluded that isothermal microcalorimetry showed the advantages of high sensitivity and precision in detecting the antibacterial activity of different antibiotics in vitro in real time [28].

In order to explore the application of Isothermal titration microcalorimetry (ITC) on the screening and identification of plant hormone receptors, Zhang et al., (2015) taken the plant hormone abscisic acid (ABA) receptor as an example, and the thermodynamic parameters of the binding of ABA receptor PYR1 to ABA was obtained by ITC test, mainly including the Binding Constant (KD), Stoichiometric Number (N) and Enthalpy of the Reaction (Δ H). ITC results showed that the binding of receptor protein between PYR1 and ABA generated the thermodynamic parameters of KD, N and Δ H to be 67 μ Mol / L, 0.92, and 19.78kj/mol, respectively, indicating the binding characteristics of specificity, saturation and high affinity, respectively as well. This conclusion supported that isothermal titration microcalorimetry could be used to effectively screen and identify hormone receptors [29].

3.6. Fluorescence spectrum

After some substances are irradiated by the certain wavelength of incident light, the

molecules are excited from the background state S_A to the excited state S_b, but the excited electrons subsequently emit energy in a very short time, returning to S_A from S_b, and part of the energy is released in the form of fluorescence with a longer wavelength than the incident light. Excitation spectrum reflects the emitted fluorescence of a substance after it is excited, in response to external excitation radiation, and mainly measures the relationship between its own emitted fluorescence wavelength and the external excitation wavelength. There is a mirror symmetry relationship between the absorption spectrum and the emission spectrum. The position of the maximum fluorescence intensity in the emission spectrum is called λ_{max}, which is an important parameter of the fluorescence spectrum [15][16][9].

Fluorescence lifetime refers to the decay law of the fluorescence intensity of molecules with time after the external excitation light is stopped, which conforms to the exponential characteristics [9].

$$I_t = I_0 e^{-kt}$$

I_0 is the maximum fluorescence intensity at excitation, I_t is the fluorescence intensity at time t, and K are the attenuation constants [9].

Quantum yield represents the efficiency of a substance in emitting fluorescence, which is defined as the ratio of the emitted quantum number to the absorbed quantum number, also known as fluorescence efficiency [9].

Fluorescence intensity F is the sum of the fluorescence intensity emitted in all directions. In fact, the instrument collects only a small part of it. The fluorescence intensity is related to the extinction coefficient of the sample at the wavelength λ_A, and the extinction coefficient is closely related to the wavelength λ_E of the excitation light, so the fluorescence intensity is determined by the wavelength of the excitation light [9].

Fluorescence polarization refers to the phenomenon that the fluorescence emitted by a fluorescent substance after receiving excitation light is polarized, which means that the plane formed between the incident excitation light angle and the fluorescence emission angle is asymmetric. This degree of polarization can be consequently used to determine the shape, size and mobility of molecules [9].

Chen (2017) designed several biofluorescent probes to discover the transfer signal across the membrane, which helped to screen anticancer drugs. Firstly, based on the configuration changes before and after the binding of nucleic acid aptamer to adenosine triphosphate (ATP), a functional nucleic acid biofluorescent probe anchored on the cell membrane was constructed to detect the release process of ATP. Cy3 and biotin molecules were labeled at the 5 ′ end and 3 ′ end of the aptamer, respectively, and hybridized with another SS DNA modified with Cy5 at the 3 ′ end to obtain a

hybrid chain with fluorescence energy resonance transfer (FRET) signal. The biotin labeled phospholipid was spontaneously inserted into the cell membrane at low temperature, and then the hybrid chain was modified on the phospholipid by the biotin streptavidin (SA) cross-linking method, which allowed to anchor the functional nucleic acid biofluorescent probe on the cell membrane; According to the mechanism that the fluorescence energy of glutathione protected gold nanoclusters (AU NCS) was selectively quenched by h ROS, a composite fluorescent nano-probe was designed to discover the living cell imaging method of spontaneous generation of h ROS when cells were stimulated by external stimuli. Streptavidin was modified on the surface of silicon nanoparticles doped with dyes (the excitation and emission peaks were at 405nm and 435nm, respectively). Correspondingly, Au NCS were modified with biotin loaded membrane penetrating peptide (CPP) in the same method. Two kinds of nanomaterials were combined by biotin streptavidin crosslinking method to form a composite Nanofluorescent probe with single excitation and double emission properties, which entered the cell spontaneously due to the action of transmembrane peptide. When the probe encountered h ROS, the fluorescence intensity of Au NCS decreased at 565nm while the fluorescence intensity of silicon nanoparticles as an internal reference was unchanged at 435nm, which were effectively and efficiently identified; Finally, based on the principle that the dye labeled nucleic acid aptamer was easily adsorbed on the surface of graphene oxide and the fluorescence was quenched, a PEGylated graphene oxide nucleic acid aptamer responding to cytochrome c biological fluorescence nanocomposite probe was developed. By using chemical crosslinking agent EDC / suflo NHS, PEG molecules with diamino group and molecular weight of 1500 were covalently crosslinked on the surface of graphene oxide, and folate molecules were modified on the amino group at the other end of PEG molecules. Subsequently the nucleic acid aptamer recognizing cytochrome C was adsorbed. The fluorescence activated imaging process of directly tracing cytochrome c release from mitochondria to cytoplasm was realized for the first time by this designed probe [30].

Sun (2022) studied the spectral properties of silicon-based coumarin, and successfully applied probes of sic-az2 and hsa-7 on biological fluorescence imaging, which detected hydrogen sulfide ultra and human serum albumin respectively. Synthesis of silicon-based coumarin derivatives was a typical small molecule with D - π - a push-pull electronic structure which was modified to design various fluorescence probes, and the influence of photostability and solvation effect on the spectra of silicon coumarin derivatives was also investigated. By hybridizing different functional groups, the photophysical and chemical properties of silicon-based coumarin were controlled, including fluorescence emission wavelength, aggregation and depolymerization properties, and photostability. In this work, a series of silicon-based coumarin small molecule fluorescent probes hsa1-7 was designed and synthesized with high selectivity and high fluorescence response signal. The fluorescence intensity of probe hsa1-7 was significantly enhanced after binding with HSA. Further, three silicon-based coumarin fluorescent probes (SiC AZS) with ultrafast kinetics was

designed to detect H_2S in vivo, showing ultra fast kinetics (25 s), wide linear range (5.0-450.0 μ M) , and a lower detection limit (0.30 μ M) [31].

3.7. Circular dichroism

An optical rotation spectrum is the novel technology which is applied to deduce the configuration and conformation of asymmetric molecules. Absorption coefficients of optically active substances for left-handed and right-handed circularly polarized light, which constitutes plane polarized light (ε), is asymmetric, ε L ≠ ε R, defined as circular dichroism (CD). If the wavelength of plane polarized light with different wavelengths λ is the abscissa, taking the difference of absorption coefficient Δε = εL-εR as the ordinate axis, and the obtained spectrum is the circular dichroic (CD) spectrum [17].

Further more, because ε L is not equal to ε R, the transmitted light does not display as plane polarized light, but becomes elliptical polarized light. The relation between molar ellipticity [θ] and Δε is:[θ]= 3300 Δε. Circular dichroism can also be plotted with the molar ellipticity as the ordinate and the wavelength as the abscissa. Because there are positive and negative values in Δε, so circular dichroism correspondingly has positive circular dichroism with peak and negative circular dichroism with valley. Circular dichroism and optical rotation spectrum are measured in the UV-Vis region, which aims to infer the configuration and conformation of organic compounds [17].

The conformational variation in wheat polygalacturonase inhibitor protein (PGIP) under the influence of different pH and temperature were examined and compared by circular dichroism (CD spectrum). The CD spectrum of natural wheat PGIP showed a single negative peak at 211 nm, under this condition wheat PGIP contained 43.7% of β Folding and 13.1% of α Helix respectively, firstly reported as the secondary structure of wheat PGIP. The bio-activity of wheat PGIP caused by pH and temperature were closely related to the parameter changes in CD spectrum. The less the bio-activity, the smaller the peak of CD spectrum. When the activity was completely lost, the negative peak shifted into blue. According to the calculation value [θ], it was found that β Folding was significantly related to the activity of PGIP in wheat [32].

Circular dichroism spectrometry was used to examined the Circular dichroism spectra of α-amylase and lipase, which studied the effect of electric field on the conformation of bio-macro-molecules, especially on its secondary structure. After being treated by electric fields of different intensities for a certain duration, the content of secondary structure of α-amylase and lipase changed in different degrees. The variation was non monotonic (oscillation) and the variation trend and degree differed between different types. The secondary structure of α-amylase changed significantly when the electric field intensity was set as 2.0kv/cm and 4.0kv/cm, while the secondary structure of lipase changed significantly when the electric field intensity was 1.5kv/cm, 2.0kv/cm and 4.5kv/cm, respectively [33].

3.8. Scanning tunneling microscope

Scanning tunneling microscope (STM), as a scanning probe microscopy tool created by Gerd Binnig and Heinrich Rohrer, allows scientists to observe and locate individual atoms with higher resolution than its equivalent atomic force microscope. In addition, the scanning tunneling microscope can precisely manipulate atoms at low temperature (4K), becoming an important measurement tool and processing tool in nanotechnology. The macro structure of the needle tip possesses the high bending resonance frequency, so as to reduce the phase lag and improve the acquisition speed. If there is only one stable atom at the tip of the needle rather than multiple needle tips, the tunnel current turns to be very stable obtaining the atomic level resolution image. If the chemical purity of the needle tip is high, a series of potential barriers are not involved [34][9].

Since the 1990s, STM has been used to study the structure of biological macromolecules, especially in revealing the structure of nucleic acid, an important genetic material. For example, Bai Chunli (1990) successfully observed the existence of triple stranded DNA by STM technology [37]. Zhang et al., (1993) effectively obtained the plasmid pBR322 DNA images by STM with higher stability in results [38].

Scanning tunneling microscopy (STM) was used by Gao et al.,(1998) to directly observe both periodic ordered and disordered regions in cotton fiber at the nano level with a diameter of 2-4nm, which composed of cellulose molecular chains arranged in parallel along the long axis. At bigger scale, the micro fibrils showed a diameter of 10-25nm, aggregated into fibrils that were alternately arranged by the basic fibrils. STM technology also directly investigated the whole enzyme molecular image of exoglucan cellobiose hydrolase, supporting the study on the dynamic process of enzyme molecules acting on cellulose [36].

3.9. Surface plasmon resonance

Surface plasmon resonance (SPR) is a physical phenomenon that when the incident light is incident on the interface of two media with different refractive indexes (such as the gold or silver coating on the glass surface) at a critical angle, it causes the resonance of metal free electrons. Due to the resonance, the electrons absorb light energy, and the reflected light is greatly weakened within a range of incident angles. The incident angles at which the reflected light completely disappears within a range of incident angles is called the SPR angle. SPR varies with the refractive index of the surface, which is in direct proportion to the mass of biomolecules bound on the metal surface. Therefore, the specific signal of the interaction between biomolecules is determined by acquiring the dynamic change of SPR angle during the biological reaction. Based on SPR principle, a new biosensor analysis technology showing biomolecular interaction is developed, which does not require to label or purify various biological components. Under natural conditions, real-time, in-situ and

dynamic measurement of various biomolecules such as polypeptides, proteins, oligonucleotides, oligoglycans, and the interaction process between viruses, bacteria, cells and small molecule compounds are carried out by sensor chips [35][9].

The local surface plasmon resonance (LSPR) effect leads the noble metal nanoparticles to show rich color changes in the visible light range, and this color change can be easily controlled by changing the shape, size, composition and surrounding media environment of the noble metal particles, based on which LSPR-ELISA was constructed by combining this controllable color development with the traditional enzyme-linked immunosorbent assay (ELISA). Compared with the traditional ELISA, it showed the advantages of high sensitivity, rapidity, portability and high reliability [40].

A canine distemper virus (CDV) immuno-sensor on the basis of etched Fiber Bragg Grating (FBG) of local surface plasmon resonance (LSPR) was designed and prepared by Zhang (2022). In view of the weak interaction between the evanescent field of FBG and the external environment, the grid region of FBG was etched with hydrofluoric acid (HF), and then a layer of Au NS particles was coated on the surface of FBG, so that the CDV antibody was consequently modified to obtain the etched FBG LSPR immuno-sensor, which was applied to the detection of canine distemper virus. The experimental results showed that the sensitivity of the sensor for detecting CDV antigen, the saturation concentration, the detection limit and the detection range were ~ - 0.046d B / log (mg / ml), ~ 10 μ G / ml, less than 50 pg / ml, and 50 pg / ml ～ 10 μ g/ml, respectively. In addition, the control detection experiments were also carried out using avian influenza (H9N2) antigen solution, rabies virus (RV) antigen solution, Newcastle disease (ND) antigen solution and CDV antigen solution as to compare and contrast, showed that the etched LSPR FBG biosensor still possessed better specificity and clinical specificity even in complex environments [39].

Table 1. Summary of application of structural biology technology on case studies.

	Structural Biology Technology	Application Examples
1	X-ray diffraction	Acetylation structure, a post-translational modification of protein [18]
2	X-ray diffraction	The spatial arrays of collagen fibrils and apatite crystals [19]
3	Coherent X-ray diffraction imaging (CXDI)	Non-crystalline bio-particles at resolution from micrometer to sub-micrometer [21]
4	Nuclear magnetic resonance (NMR)	Two polypeptides that were important to cell membrane fusion and transmembrane signal in transduction function [22]
5	Nuclear magnetic resonance (NMR)	The cloning, expression and purification of UBX domain of human UBXD2 protein [23]
6	Electron microscope three-dimensional reconstruction	Pral, as an endogenous complement protein inhibitor expressed by *Candida albicans* [24]
7	Electron microscope three-dimensional reconstruction	Human adenovirus capsid 3.4 Å [25]
8	Biological mass spectrometry	The protein expression between normal leukocytes and acute leukemia (AL) cells [26]
9	Biological mass spectrometry	The diagnosis of esophageal cancer [27]
10	Microcalorimetry	Real-time determination of antibacterial effects in vitro [28]
11	Microcalorimetry	Screening and identification of plant hormone of abscisic acid (ABA) receptors [29]
12	Fluorescence spectrum	The transfer signal across the membrane, which helped to screen anticancer drugs [30]
13	Fluorescence spectrum	Hydrogen sulfide ultra and human serum albumin [31]
14	Circular dichroism	The conformational variation in wheat polygalacturonase inhibitor protein (PGIP) under the influence of different pH and temperature [32]
15	Circular dichroism spectrometry	Secondary structure of α-amylase and lipase [33]
16	Scanning tunneling microscope (STM)	Triple stranded DNA [37] ; Plasmid pBR322 DNA [38]
17	Scanning tunneling microscope (STM)	Both periodic ordered and disordered regions in cotton fiber at the nano level [36]
18	Surface plasmon resonance (SPR)	A canine distemper virus (CDV) immuno-sensor [39]

4. Conclusion and Future Research

As can be seen in Table 1, so far fewer studies have investigated the structural biology on genomes, while the majority of structural biology cases choose proteins as research targets. However, the deficiencies / research gaps of DNA sequencing technology has been critically discussed in my previous paper [41], which requires structural biology methods to fill in this research gaps, and a convenient tool of observing DNA molecules has been designed in my previous article as well [42]. The details are below:

Theory

Nowadays, for the analysis of genetic similarity in species or subspecies by DNA sequencing technology, the selected DNA sequence fragments from gene bank only reveals a small part of the genetic information compared with the total genetic information contained by the whole genomes. Therefore, the significant difference derived from very limited/bias genetic information is likely to be a misleading conclusion. There are several reasons:

First, using DNA sequence fragment primers to amplify the chemical reaction, the information obtained is only the repetitive primer sequences of gene fragments and its relative molecular weighted among the total tested gene sequences in a experiment, but it does not reflect the spatial arrangement and combination information of various sequences on the genome. However, the arrangement and combination information of different gene sequences in the genomes is the main contribution factor of genetic variation, because most of the gene sequences revealed by DNA primers are highly conserved sequence fragments in the evolutionary process. Its own changes of DNA sequences are rare, which mainly depends on the change of arrangement and combination of various conserved sequences to achieve genetic variation in reproduction process for a population.

Secondly, in the past research, ovum cell and sperm cell are seldom separately distinguished to analyze each genetic contribution rate to their offspring. The mass/weight of DNA molecules in egg cells is much larger than DNA in sperm cells, so the genetic contribution rate of maternal DNA to offspring DNA is significantly higher than that of sperm suppliers. Consequently, statistic classification of genetic variation must input this statistic factor to distinguish. In comparison, the genetic contribution rate of bio-electromagnetic waves (life signal waves) by sperm supplier to offspring is much higher than maternal parents (I have discussed this in biophysics articles).

Consequently, because the amount of genetic information tested by gene sequencing technology accounts for limited/bias proportion of the total genetic information of the genome, the significant difference in results reflected by multivariate statistics is

likely to be a misleading conclusion.

Methods

1. The common methods used as chromosome binding technology mainly include Centromere Binding Technology (C-Binding), Guinacrine Binding Technology (G-Binding), Giemsa Binding Technology (G-Binding), Reverse Binding Technology (R-Binding), etc. These chromosome binding technologies are designed on the basis of the various staining chemicals [1], which reflect different regions or functions in chromosome. In my article, DAPI fluorescence binding technology, which results in the appearance of AT rich region on chromosome, is selected as an example of designing a new method in observing the structure of DNA molecules at three dimensions:

If the slide glass is the horizontal plane, and the vertical line is the eyesight line of microscope for DNA molecule observation, then the angle between the planes of AT DNA sequences and the eyesight line observed by microscope is $\pm \alpha$ ($0° \leq \alpha \leq 90°$), and α is generally uniform in the DNA molecules of a species, but varies among different species. If this angle tends to be zero, then the DAPI binding tends to be not observed; If this angle tends to be 90°, then the DAPI binding tends to be more clearly observed by florescence microscope. The structure of DNA molecules can be consequently deduced by the clearness of fluorescence binding. Despite of fluorescence polarization, it is expected to obtain the reliable and re-occurring results when the other experiment conditions remains constant.

Consequently, it is to classify the DNA samples by the molecular cytogenetic karyotype using FISH technology firstly, based on which the DNA molecular structure is further deduced according to the clearness of fluorescence binding. Then this structural biology is correlated to the functional groups of biological traits (such as pathological characters or immunological characters) as bio-markers.

Step 1. The molecular cytogenetic karyotype of chromosomes is analyzed by fluorescence in situ hybridization (FISH) technique;

Step 2. These chromosomes examined in experiment are classified by multivariate cluster analysis and genetic distance analysis on the basis of molecular cytogenetic karyotype, preliminarily leading to different families of chromosomes.

Step 3. Within each family of chromosomes, the DNA molecular structure of each chromosome is deduced according to the clearness of fluorescence binding described above. Then it is further to classify different sub-families of chromosome by this structural biology marker.

Step 4. Each sub-family of chromosome is correlated with the functional groups of biological traits (such as pathological characters or immunological characters) as

bio-markers.

In order to quantify the clearness of fluorescence binding, the spectrometer is used to measure the fluorescence intensity of each spectral line on fluorescence binding. More chromosome binding showing other base pairs (such as GC base pair) are selected to compare with AT-rich base pair for further analysis.

There are some further improvements in future methods:
Firstly, various fluorescence binding probes which reveal different DNA fragments need to be designed by hybridizing different functional groups as comparison and contrast in this research, to meet different needs;

Secondly, to further quantify the parameters of fluorescence spectrum, fluorescence lifetime, fluorescence intensity, fluorescence efficiency and fluorescence polarization which have been discussed above are examined on the basis of designed fluorescence binding probes, to improve the accuracy of this research. Nevertheless there is a trade-off between the experiment cost and DNA classification scales.

Enzyme structural biology

In addition to the structural genome studies, my another functional genome study paper [43] has designed a new method to identify the specific enzyme species within an isozyme family at the molecular weight level expressed as specific gene trait, which can be separated and collected in electrophoresis pipes to conduct further structural biology study for bio-medicine production purpose. Firstly, to further study the function of this specific enzyme species in cells, the biofluorescent probes will be designed according to the functional groups of isozyme family used in gene screening procedure of my functional genome study paper. Fluorescence spectrum technology which is illustrated in above case studies should be applicable in this step. After this, the tertiary structure of this enzyme species can be further studied according to other technologies illustrated in above case studies, and the selection of technology is depended on the needs of bio-medicine production, availability of facilities and economic cost. After all, multiple technologies can be applicable on the study of tertiary structure in enzyme molecules illustrated in above case studies, including X-ray diffraction, Nuclear magnetic resonance (NMR), Coherent X-ray diffraction imaging (CXDI), Electron microscope three-dimensional reconstruction, Circular dichroism spectrometry, Scanning tunneling microscope (STM) etc.

This journal article is previously published as: Liu Huan. (2022). Article 19. Essay: Structural Molecular Biology. Journal of Environment and Health Science (ISSN 2314-1628), 2022(08)., which is converted into Journal of Biological Sciences (ISSN 2958-4035). Both Journals belong to the same publisher, Liu Huan. The previous journal article is closed to the public, but the previous reference is still valid. Latest revised on 26/04/2023; 30/05/2023; 05/06/2023.

References:

[1] 结构生物学。搜狗百科。
[2] DNA 一级结构。搜狗百科。
[3] DNA 二级结构。搜狗百科。
[4] DNA 三级结构。搜狗百科。
[5] 蛋白质一级结构。搜狗百科。
[6] 蛋白质二级结构。搜狗百科。
[7] 蛋白质三级结构。搜狗百科。
[8] Textbook of Structural Biology. Anders Liljas etc. 苏晓东译。科学出版社。ISBN 978-7-03-036392-3.
[9] 《结构生物学》，梁毅主编。ISBN 7-03-014427-9。
[10] 晶体 x 射线衍射。搜狗百科。
[11] 核磁共振原理。搜狗百科。
[12] 电镜三维重构技术。搜狗百科。
[13] 生物质谱技术。搜狗百科。
[14] 生物微热量仪。搜狗百科。
[15] 荧光光谱。搜狗百科。
[16] 激发光谱。搜狗百科。
[17] 圆二色光谱。搜狗百科。
[18] 施玲玲. 大肠杆菌转乙酰酶 ElaA 的结构和功能研究[D].中国科学技术大学,2018.
[19] Adriana Bigi, Manfred Burghammer, Rosanna Falconi, Michel H.J Koch, Silvia Panzavolta, Christian Riekel,Twisted Plywood Pattern of Collagen Fibrils in Teleost Scales: An X-ray Diffraction Investigation, Journal of Structural Biology, Volume 136, Issue 2, 2001, Pages 137-143, ISSN 1047-8477. https://doi.org/10.1006/jsbi.2001.4426
[20] Parker, M. Protein Structure from X-Ray Diffraction. *Journal of Biological Physics* **29,** 341–362 (2003). https://doi.org/10.1023/A:1027310719146.
[21] Amane Kobayashi (小林周)1,2, Yuki Sekiguchi (関口優希)1,2, Yuki Takayama (高山裕貴)2, Tomotaka Oroguchi (苳口友隆)1,2, Keiya Shirahama (白濱圭也)1, Yasufumi Torizuka (鳥塚康史)3, Masahiro Manoda (間野田昌広)3, Masayoshi Nakasako (中迫雅由)1,2, a), and Masaki Yamamoto (山本雅貴). TAKASAGO-6 apparatus for cryogenic coherent X-ray diffraction imaging of biological non-crystalline particles using X-ray free electron laser at SACLA .Review of Scientific Instruments 87, 053109 (2016); https://doi.org/10.1063/1.4948317.

[22] 曾丹云. 杆状病毒膜融合蛋白 HaF 融合肽和钾离子通道调节剂 ImKTx104 的核磁共振结构研究[D].中国科学院研究生院（武汉物理与数学研究所）,2012.
[23] 吴清林. UBXD2 UBX 结构域结构与功能研究和核磁共振方法研究树枝形分子与生物表面活性剂相互作用及基于树枝形分子的药物筛选[D].中国科学技术大学,2010.
[24] 刘颖. 白色念珠菌重要毒性因子的电镜结构生物学研究[D].兰州大学,2020.DOI:10.27204/d.cnki.glzhu.2020.003422.
[25] 宋双林. 基于冷冻电镜局部重构的腺病毒结构研究[D].湖南师范大学,2020.DOI:10.27137/d.cnki.ghusu.2020.000902.
[26] 张学敏,王杰,崔久嵬,王冠军,何昆,靳宝锋,王红霞,于鸣,胡美茹,李慧艳,李爱玲,沈倍奋. 生物质谱技术应用于人急性白血病临床分型诊断[C]//.中国分析测试协会科学技术奖发展回顾.,2015:236.
[27] 刘清银,孙良起,涂斌.基于磁珠分离的生物质谱技术用于食管癌临床诊断[J].世界华人消化杂志,2012,20(31):3021-3026.
[28] 王伟霞,卢葵,徐艳超,靖红艳,刘浩,姚俊霞.等温微量热技术比较原研和仿制头孢曲松钠体外抑菌效果（英文）[J].中国抗生素杂志,2020,45(09):893-900.DOI:10.13461/j.cnki.cja.006963.
[29] 张卿,邢宇,郝敬虹,曹庆芹,秦岭.基于等温滴定微量热技术的植物脱落酸受体鉴定的方法[J].北京农学院学报,2015,30(04):20-23.DOI:10.13473/j.cnki.issn.1002-3186.2015.0087.
[30] 陈婷婷. 生物荧光探针在活细胞成像中的研究与应用[D].湖南大学,2015.
[31] 孙琰. 硅基香豆素在硫化氢和人血清白蛋白生物成像中的应用[D].华东师范大学,2021.DOI:10.27149/d.cnki.ghdsu.2021.001017.
[32] 万琳,周立.小麦 PGIP 圆二色性与生物活性关系[J].应用与环境生物学报,2001(05):434-437.
[33] 姚占全. 应用圆二色光谱研究电场对蛋白质（酶）构象的影响[D].内蒙古大学,2005.
[34] 扫描隧道显微镜。搜狗百科。
[35] 等离子表面共振。搜狗百科。
[36] 高培基,刘洁,张玉忠,曲音波,庞世瑾.天然纤维素在生物降解过程中超分子结构的变化——氢键断裂在纤维素降解中作用的探讨[J].自然科学进展,1998(04):9-15.
[37] 白春礼、叶坚、龚立三等，科学通报。1990,3S（24）：1841-1842.
[38] 张平城,王中怀,白春礼,黄熙泰.超螺旋 pBR322 DNA 的 STM 研究[J].科学通报,1993(16):1532-1534.
[39] 张杨. 基于腐蚀型光纤 Bragg 光栅的局域表面等离子体共振犬瘟热病毒免疫传感器研究[D].重庆理工大学,2022.DOI:10.27753/d.cnki.gcqgx.2022.000840.
[40] 申珣,翁国军,李剑君,朱键,赵军武.局域表面等离子体共振酶联免疫法的显色方法及检测应用[J].分析科学学报,2021,37(03):388-394.DOI:10.13526/j.issn.1006-6144.2021.03.021.
[41] Liu Huan (2021), Discussion on Gene Sequencing and Classification of DNA Genetic Markers. Journal of Environment and Health Science (ISSN 2314-1628). https://doi.org/10.58473/JBS0019
[42] Liu Huan (2021), The Application of Spectral Informatics on the Genetic

Marker/光谱信息及其在遗传标记技术的应用. Journal of Environment and Health Science (ISSN 2314-1628). https://doi.org/10.58473/JBS0003
[43] Liu Huan (2023). Original review of specificity in the interaction between pathogen invasion and host organism. Journal of Biological Sciences (ISSN 2958-4035). 2023 (04). https://doi.org/10.58473/JBS0022
[44] Cryo-EM structure of human Pol κ bound to DNA and mono-ubiquitylated PCNA.Lancey C , Tehseen M , Bakshi S , Percival M , Takahashi M , Sobhy MA, Raducanu VS , Blair K , Muskett FW , Ragan TJ , Crehuet R , Hamdan SM , De Biasio A. Nat Commun 12 (2021).PMID: 34667155.
https://doi.org/10.1038/s41467-021-26251-6
[45]. CryoEM single particle dataset for NanR dimer-DNA hetero-complex Venugopal H , Horne CR , Panjikar S , Wood DM, Henrickson A , Brookes E, North RA, Murphy JM , Friemann R , Griffin MDW , Ramm G , Demeler B , Dobson RCJ Nat Commun 12 (2021). PMID: 33790291.
https://doi.org/10.1038/s41467-021-22253-6
[46]. Cryo-EM structures and biochemical insights into heterotrimeric PCNA regulation of DNA ligase Sverzhinsky A , Tomkinson AE , Pascal JM Structure 30 371-385.e5 (2021); PMID: 34838188.https://doi.org/10.1016/j.str.2021.11.002
[47]. Structures of a mobile intron retroelement poised to attack its structured DNA target Chung K , Xu L , Chai P , Peng J , Devarkar SC , Pyle AM
Science 378 627-634 (2022); PMID: 36356138
https://doi.org/10.1126/science.abq2844
[48]. Andrii Iudin and others, EMPIAR: the Electron Microscopy Public Image Archive, Nucleic Acids Research, Volume 51, Issue D1, 6 January 2023, Pages D1503–D1511, https://doi.org/10.1093/nar/gkac1062
[49]. Structure of the Dicer-2-R2D2 heterodimer bound to a small RNA duplex Yamaguchi S, Naganuma M, Nishizawa T , Kusakizako T , Tomari Y , Nishimasu H , Nureki O. Nature 607 393-398 (2022). PMID: 35768503
https://doi.org/10.1038/s41586-022-04790-2
[50]. Cryo-electron microscopic structure of the nucleoprotein-RNA complex of the European filovirus, Lloviu virus. Hu S , Fujita-Fujiharu Y , Sugita Y , Wendt L , Muramoto Y , Nakano M , Hoenen T , Noda T. PNAS Nexus (2023)
https://doi.org/10.1093/pnasnexus/pgad120
[51]. Structural and mechanistic basis for recognition of alternative tRNA precursor substrates by bacterial ribonuclease P. Zhu J, Huang W , Zhao J, Huynh L, Taylor DJ , Harris ME. Nat Commun 13 (2022). PMID: 36045135
https://doi.org/10.1038/s41467-022-32843-7
[52]. Epoxidized graphene grid for highly efficient high-resolution cryoEM structural analysis.Fujita J , Makino F , Asahara H , Moriguchi M , Kumano S, Anzai I , Kishikawa J , Matsuura Y , Kato T , Namba K , Inoue T. Sci Rep 13 (2023) PMID: 36755111. https://doi.org/10.1038/s41598-023-29396-0
[53].A monoclonal antibody that neutralizes SARS-CoV-2 variants, SARS-CoV, and other sarbecoviruses.Wang P , Casner RG , Nair MS , Yu J, Guo Y, Wang M, Chan JF , Cerutti G , Iketani S , Liu L, Sheng Z, Chen Z , Yuen KY , Kwong PD, Huang Y,

Shapiro L , Ho DD. Emerg Microbes Infect 11 147-157 (2022).PMID: 34836485
https://doi.org/10.1080/22221751.2021.2011623
[54].The tethered peptide activation mechanism of adhesion GPCRs
Barros-Álvarez X , Nwokonko RM, Vizurraga A, Matzov D, He F , Papasergi-Scott MM , Robertson MJ , Panova O , Yardeni EH, Seven AB, Kwarcinski FE, Su H, Peroto MC, Meyerowitz JG , Shalev-Benami M, Tall GG , Skiniotis G
Nature 604 757-762 (2022). PMID: 35418682
https://doi.org/10.1038/s41586-022-04575-7
[55]. Structure of a RecT/Redβ family recombinase in complex with a duplex intermediate of DNA annealing.Caldwell BJ, Norris AS, Karbowski CF , Wiegand AM, Wysocki VH , Bell CE. Nat Commun 13 (2022).PMID: 36543802
https://doi.org/10.1038/s41467-022-35572-z